

Physicochemical Properties of Hybrid Biodegradable Silica-Hydrogel Composites

Adhemar Watanuki Filho^{a,b*} , Uilian Gabaldi Yonezawa^a, Marcia Regina de Moura^a,

Fauze Ahmad Aouada^a

^aUniversidade Estadual Paulista (UNESP), Faculdade de Engenharia, Departamento de Física e Química, Grupo de Compósitos e Nanocompósitos Híbridos (GCNH), Avenida Brasil, 56, Centro, 15385-000, Ilha Solteira, SP, Brasil.

^bInstituto Federal de Educação, Ciência e Tecnologia de São Paulo (IFSP), Departamento de Construção Civil, Alameda Tucuruí, 164, Zona Norte, 15385-000, Ilha Solteira, SP, Brasil.

Received: January 16, 2023; Revised: April 14, 2023; Accepted: June 05, 2023

Hydrogels based on polyacrylamide, carboxymethylcellulose and silica are composites with good absorption and release properties over time, and this behavior allow their application in several areas. Thus, the aim of study was to analyze the absorption kinetic, spectroscopic, morphological, and structural properties of hydrogels prepared using different silica concentrations (0, 0.5, and 2.5%). The results showed that the swelling degree reduces with increasing silica, i.e., there was increase in crosslinking density, which was confirmed by SEM images. The reductions in the swelling degrees at equilibrium were 26.19% (0.50% silica) and 22.02% (2.5% silica) when compared to PAAm+CMC hydrogel. FTIR spectra showed characteristic spectroscopic bands of silica between 1384 and 1120 cm^{-1} indicating that its incorporation into the hydrogel matrix has occurred, which was also observed in the XRD diffractograms. Thus, the study of biodegradable hybrid hydrogels is relevant because they can potentially be applied in areas such as agriculture, tissue engineering and even civil construction.

Keywords: Composite, hydrogel, polymer absorbent, silica.

1. Introdução

Polyacrylamide (PAAm) and carboxymethylcellulose (CMC) hydrogels containing silica are considered to be three-dimensional hybrid crosslinked, hydrophilic composites with high absorption capacity and release characteristics over time^{1,2}. Dragan and Apopei³ reports that these types of polymers to increase mechanical strength and swelling response, should be designed as multicomponent networks, i.e., as interpenetrating polymer networks (IPNs) or semi-IPN.

The IPNs are combinations of cross-linked polymers, at least one of them being synthesized and/or cross-linked within the immediate presence of the other⁴, without any covalent bonds between them, which cannot be separated unless chemical bonds are broken³. Myung et al.⁴ report that are created for the purpose of conferring key attributes of one of the components while maintaining the critical attributes of another, sometimes the properties are exhibited by the IPN that are not observed in either of the two single networks alone.

IPN hydrogels can be classified as simultaneous IPN, when the precursors of both networks are mixed and the two networks are synthesized at the same time by independent, non interfering routes such as chain and stepwise polymerization³ and sequential IPN, typically performed by swelling of a single-network hydrogel into a solution containing the mixture of monomer, initiator and activator, with or without a cross-linker⁵. If a cross-linker is present,

fully-IPN result, while in the absence of a cross-linker, a network having linear polymers embedded within the first network is formed (semi-IPN)³.

Semi-IPNs, on the other hand, are compositions in which one or more polymers are crosslinked and one or more polymers are linear or ramified⁵. Dragan and Apopei³ affirm that semi-IPNs also are a type of interpenetrating polymer network (IPN) hydrogel in which one component has a linear instead of a network structure. Semi-IPNs have been shown to offer advantages such as improved mechanical properties when compared to single-network hydrogels, and these type of hydrogel can be formed by combining two different polymers, one in the cross-linked form and one in the linear form⁶.

These polymers can be synthesized from synthetic, semi-synthetic, or natural raw materials, whose main function is to absorb large amounts of water or other organic fluids for later release². Others authors define hydrogels as polymeric systems that show the capability of swelling in water and retaining a significant fraction (>20%) of water inside their three-dimensional structure, without dissolving in water^{7,8}.

Thus, polyacrylamide (PAAm) and carboxymethylcellulose (CMC) hydrogels containing silica can be considered as multicomponent systems, i.e., as semi-IPNs systems, since only the PAAm is crosslinked and entangled with the non-crosslinked CMC polysaccharide in the polymer network. Importantly, the network properties can be tailored by the type of polymer and its concentration, by the applied crosslinking method as well as by the overall procedure used for their

*e-mail: watanuki@ifsp.edu.br

preparation. In many cases, polysaccharides are selected for the formation of IPN hydrogel networks, which are either chemically or physically crosslinked. Sometimes both entangled macromolecules are based on polysaccharides, but often also combinations of synthetic polymers together and polysaccharides chains are used to create (semi)-IPNs⁹.

Hydrogels can be classified as hydroretentor material¹⁰ and the swelling process of a hydrogel is governed by physical factors intrinsic to the three-dimensional network and external factors¹¹. Some physical factors, such as the presence of hydrophilic groups, (-OH-, -NH₂-, -COOH-, -CONH₂-, -SO₃H-) in the polymer chain structure, lower crosslinking density and high flexibility of the polymer network, contribute satisfactorily to a swelling degree higher of the material¹². It is emphasized that the water storage occurs from the polymeric chain expansion due to repulsion from the hydrophilic groups on the polymeric chains^{13,14}. Thus, this characteristic justifies the use of these polymers in the fields of agriculture, medicine, construction, and others.

For the construction field, Bose et al.¹⁵ state that cement pastes cured internally with acrylamide-rich composite hydrogel particles showed higher growth of hydration products in hydrogel-related voids compared to conventional (silica-free) hydrogel pastes¹⁶. Thus, polyacrylamide-silica composite hydrogel particles appear to have an advantage over conventional superabsorbent polymers (SAPs) by promoting pozzolanic reactions in vicinity of the SAP-related voids while continuing to facilitate internal curing¹⁶.

For the agriculture, most of the hydrophilic hydrogels are destined as soil conditioners and nutrient carriers, and can be applied when seeding or coated on the seed itself¹⁷. Bortolin et al.¹⁸ synthesized composite hydrogels based on PAAm, methylcellulose (MC) and montmorillonite (MMt) appropriate for the controlled release of nitrogenated fertilizer. The results showed that the release of fertilizer was slower for the hydrogel samples before and after hydrolyzing of the hydrogel samples, as compared with the urea without the presence of the hydrogel¹⁸.

Stealey et al.¹⁹ found that addition of nanoparticles to polymeric hydrogel has been shown to improve the retention and delivery of biologics. The authors produced a nanocomposite hydrogel with nanoclay and identified simple but effective experimental conditions to obtain sustained protein release, up to 23 times slower as compared to traditional hydrogels.

The applicability of hydrogels produced with nanosilica in water treatment was demonstrated for adsorption of metals ions from aqueous solution. For Lee et al.²⁰, the hydrogel showed a high adsorption capacity that was owed to the presence of amine groups on the nanosilica surface as well as the highly porous structure. Also, the effects of different parameters (Pb²⁺ concentration, adsorbent content, pH value, and contact time) on the adsorption capacity of the hydrogel were low. On the other hand, the electrostatic interaction between the hydrogel's carboxylate groups and the Co²⁺, Cu²⁺, Pb²⁺, and Zn²⁺ ions lead to unselectivity for removal of these metal ions from aqueous solution²¹.

However, some types of hydrogels, such as natural hydrogels, can demonstrate some limitations in mechanical properties and solute sorption, and this is not interesting when applied in some areas. An alternative is the use of silica

during hydrogel synthesis to obtain a hybrid composite, as reported in the literature¹⁵.

Thus, hydrogels synthesized from synthetic and natural polymer mixtures have been becoming an option to improve their biodegradability, mechanical properties, hydrophilicity, and others, to widen their technological application in different areas²².

Hydrogels with additions of minerals, such as clays or silica are interesting because they have advantages such as low cost and improved composite hydrogel properties such as increased thermal stability²³, absorption capacity, and water absorption rate¹⁰. Krafcik et al.²⁴ showed in their studies a novel method of incorporating amorphous nanosilica into poly(acrylic acid-acrylamide) hydrogel particles to obtain a composite hydrogel. They also showed satisfactory results with the application of the polymer in the civil construction field.

This study is based on the synthesis of composite hybrid hydrogels based on polyacrylamide, carboxymethylcellulose (CMC) polysaccharide, and silica. These polymers are composed of chemically, functionally, and morphologically distinct blocks, which can include natural, synthetic raw materials or nano/microstructures interconnected via physical or chemical means and have been developed to improve existing formulations and to expand their range of applications²⁵.

Thus, hydrogels based on polyacrylamide (PAAm) have been applied frequently in several areas (agricultural, biomedical, pharmaceutical area)²⁶ due to their properties, such as high hydrophilicity and good mechanical behavior. It is made from acrylamide (AAM) monomers, consisting of the -CONH₂ groups which has high chemical activity. Thus, PAAm hydrogels have been extensively studied for biomedical applications such as drug delivery systems²⁷.

Polyacrylamide hydrogels consist of a covalent polymer network and water; under ordinary conditions, the polyacrylamide network is stable, and water is mobile into the polymer network²⁸. Because of their mechanical properties and hydrophilicity, this type-hydrogel has been widely used as the main base in developing new types of absorbent polymers²⁹.

The application of a polysaccharide, such as CMC, has been demonstrated to be a good option for the preparation of hydrogels because it has carboxylic groups in its chemical structure that can be ionized, and these groups have higher hydrophilicity than hydroxyl groups¹⁸. The choice for silica is justified because these are additions that can potentially contribute to composite elaboration, as they can provide high thermal stability, good mechanical strength, high swelling degree, adsorption capacity and good gas barrier properties^{18,30}, just like mineral clays. Noteworthy that the gas barrier improvement is associated with the homogeneous dispersion of the inorganic material in the polymeric matrix, preferably observed in layers (intercalation) or in individual particles (exfoliation), which will promote the multiplication of the obstacles to the permeant passage, making a tortuous path, delaying permeation³¹.

Silica particles as inorganic fillers in a hydrogel network are widely used because of their tunable size, uniform structure, hydrophilic nature, and stability in aqueous solutions. Like most other inorganic fillers, the high surface to volume ratio

facilitates strong physical interactions, and efficient stress transfer. Silica particles acting like initiators can also be used to graft hydrophilic monomers and then grow chains³². Sometimes, excellent biocompatibility is a leading factor when considering the type of inorganic filler³³.

In this way, our study investigated the effect of hydrogels prepared from different concentrations of silica, 0, 0.5, and 2.5% weight (wt)/acrylamide weight (wt), on water absorption properties by swelling degree measurements, morphological, kinetic, and structural characteristics of the hydrogels, using distilled water as a swelling medium. Thus, the development of hybrid biodegradable hydrogels is relevant because the improvement of the properties of these composites expands their potential applications in areas such as agriculture, tissue engineering, and even in civil construction.

2. Experimental Procedures

2.1. Hydrogel synthesis

Three types of hybrid composite hydrogels composed of polyacrylamide (PAAm), biodegradable polysaccharide carboxymethylcellulose (CMC), and silica were obtained through free radical polymerization as showed in Figure 1, following the procedures described by Nascimento et al.¹⁰ and Aouada³⁴. These hybrid nanocomposite hydrogels were synthesized using 6.0% (wt/v) acrylamide (AAm) monomer (Sigma-Aldrich 99%, C_3H_5NO , MW = 71.08 g/mol) in an aqueous solution containing 1.0% (wt/v) of polysaccharide carboxymethylcellulose (CMC) (Synth P.A, Mv = 114.000 g/mol), different silica (Tecnosil Industria e Comércio de Produtos Químicos Ltda.) contents: 0% (reference), 0.5% and 2.5% (mass% concerning to AAm + CMC mass).

It was used 2.0% (mol relative to AAm monomer) of N'-N'-methylenebisacrylamide (MBAAm) as a crosslink agent (Sigma-Aldrich 99%, $C_7H_{10}N_2O_2$, MW = 154.17 g/mol), 6.67 mmol/L of N, N, N', N'- tetramethylethylenediamine (TEMED) (Sigma-Aldrich 99%, $(CH_3)_2NCH_2CH_2N(CH_3)_2$, MW = 116.20 g/mol) as reaction catalyst, and 3.50 mmol/L of sodium persulfate (Sigma-Aldrich > 98%, $Na_2S_2O_8$, MW = 238.10 g/mol) as reaction initiator.

To improve the efficiency of hydrogel polymerization was necessary to apply nitrogen gas (N_2), after TEMED addition,

for 10 minutes. After this stage, sodium persulfate solution was added under stirring into the polymeric solution to initiate the polymerization process. The hydrogel-forming solution was stored for 24 hours at a temperature of 25°C until complete polymerization. Hybrid nanocomposite hydrogels were subjected to the dialysis process, i.e., changing the storage water daily for 7 days to eliminate the reagents that were not consumed.

Subsequently, hydrogels were ground into microparticles and subjected to the drying process in an oven at $40^\circ C \pm 1^\circ C$ for approximately 48 hours or until achieving constant (variation < 0.50%). With the material completely dry, it was again ground and stored until its application. All concentrations of the required reagents were pre-established by our research group GCNH (Grupo de Compósitos e Nanocompósitos Híbridos)³⁵.

2.2. Swelling degree (SD)

The hydrophilic properties of nanocomposite hydrogels were determined by measuring their swelling degree (SD). The determinations were measured at room temperature ($25^\circ C \pm 1^\circ C$) by gravimetric analysis on an analytical balance (Shimadzu AUY-220-I). After the dialysis procedures, the swollen hydrogels were cut into a cylindrical shape (circles of 22 mm diameter) and dried in an oven at $40^\circ C \pm 1^\circ C$ until their constant mass (M_d). After, the dried hydrogels were placed into a vessel containing 20 mL of distilled water. Noteworthy is that the swelling measurements were performed in triplicate for each hydrogel type analyzed.

For each predetermined time (measurements every 1 hour up to 8 hours, then at 24h, 32h, 48, and 72 hours), the samples were withdrawn from swelling media, and the excess of the water surface was removed with soft paper. Then, their weights were measured using (M_t) an analytical balance (Shimadzu AUY-220-I). Immediately, the samples were again placed on the vessel. The swelling degree was determined by the ratio between the mass of swollen hydrogel at the determined time and the dry hydrogel mass, according to Equation 1.

$$SD = \frac{M_t}{M_d} (\text{g } H_2O \text{ or solution per g hydrogel}) \quad (1)$$

The measures were performed in triplicate ($n = 3$), and the error bars in the graph correspond to the standard deviation.

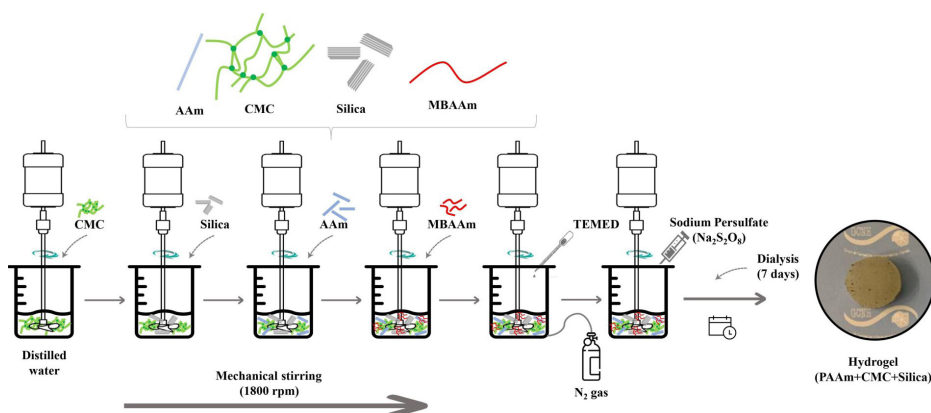


Figure 1. Schematic representation of synthesis of PAAm+CMC_Silica hydrogels.

2.3. Kinect parameters

Kinect parameters are obtained through swelling degree measures as the function of time in different solutions. For each curve, the diffusion exponent (n) and diffusion constant (k) were calculated using Equation 2³⁶.

$$\frac{M_t}{M_{eq}} = kt^n \quad (2)$$

where M_{eq} is the hydrogel mass at equilibrium time, t is the time, k is a diffusion constant (dependent on hydrogel type and swelling medium), and n is known as the diffusion exponent that supplies the kind of water absorption mechanism.

Equation 2 was applied from the initial stage until 60% of the kinetic curve, thus ensuring that the curve plotted between $\ln[(M_t)/(M_{eq})]$ versus $\ln t$ is linear³⁷. The kinetic parameters involved in the mechanism of diffusion of water towards hydrogel were determined by the slope and linear coefficients of the $\ln(M_t/M_{eq})$ versus $\ln(t)$ curve, respectively.

2.4. Fourier transform infrared spectroscopy (FTIR)

After realizing the swelling degree test, the hydrogels were macerated and dried in an oven ($40 + 2^\circ\text{C}$) for 48h or until constancy mass was verified. These dry hydrogels were comminuted manually until the powdered samples were obtained.

FTIR spectra of the nanocomposite hydrogels were recorded using a Nicolet-NEXUS 670 FTIR spectrophotometer with 2 cm^{-1} resolution. KBr pellet technique (0.5 mg of sample in 100 mg of KBr) was applied for monitoring changes in the IR spectra of the samples in the range of $4000\text{--}400\text{ cm}^{-1}$. All measurements were recorded by the accumulation of 128 scans, and the vibrational energies are reported in wavenumber (cm^{-1}).

2.5. X-ray diffraction (XRD)

X-ray diffraction (XRD) patterns of the clay, hydrogel and their nanocomposites were obtained by (Shimadzu – XDR – 6000) diffractometer using Cu-K_α radiation ($\lambda = 0.154\text{ nm}$) under a voltage of 30kV and current of 40 mA. All specimens were analyzed in continuous scan mode with 2θ ranging from 5° to 50° at a scanning rate of $1^\circ/\text{min}$. Additionally, the basal spacing or the distance of two adjacent silica platelets was determined from the position of $d(001)$ reflection, which is calculated by Bragg's equation ($n\lambda = 2.d.\sin\theta$).

2.6. Scanning electron microscopy (SEM)

Hydrogel and nanocomposite morphologies were observed by using a ZEISS EVO LS15 electronic microscope operating at an accelerating voltage of 10 kV. The samples were swollen, until the equilibrium stage (48h) at $25^\circ + 1^\circ\text{C}$, in distilled water medium. After this step, they were frozen in liquid nitrogen and freeze-dried at -55°C for 24h in a lyophilizer (model Enterprise II Terroni). Finally, the fractured nitrogen samples were gold-sputtered before SEM observation.

2.7. Statistical analysis

The experimental results for each treatment set were available by analysis of variance (ANOVA) from the Tukey test, with a 5% significance level, using SISVAR[®] software.

3. Results and Discussion

3.1. Swelling degree (SD)

The swelling curves of the silica-hydrogel composite in distilled water are shown in Figure 2. It was found that silica hydrogels reach a swollen equilibrium state after 32h. At the same time, the same equilibrium stage of hydrogel without silica was reached after 48h. All hydrogels showed water absorption in the range of 24–34 (g/g). In addition, the silica interferes directly with this hydrophilic property because the higher its concentration minor the swelling degree. This behavior can be related to the hydroxyl groups on silica particles forming a hydrogen bond with the PAAm chains, which leads to a higher crosslink density³⁸. Thus, in a dense three-dimensional network, the space capable of accommodating water molecules becomes smaller, resulting in a decrease in the swelling degree of composite silica-hydrogels^{39,40}.

In the first eight hours of testing, it was possible to observe accelerated water absorption, independently of the concentration of silica, reaching the equilibrium conditions after 48 hours. The results showed that the pure hydrogel had $SD_{\text{equilibrium}}$ equal to $33.6 \pm 0.3\text{ g/g}$. For hybrid hydrogels with 0.5% and 2.5% silica concentration, the average $SD_{\text{equilibrium}}$ values were $24.8 \pm 1.0\text{ g/g}$ and $26.2 \pm 1.7\text{ g/g}$ respectively.

The relationship between SD_{eq} and the amount of silica in the composites was shown in Figure 3.

The reduction of SD_{eq} for hybrid hydrogels (0.5 and 2.5% silica) was 26.19% and 22.02%, respectively, when compared with PAAm+CMC hydrogel. This behavior can be attributed to the presence of silica as a physical crosslinker in the polymeric matrix, which can cause a reduction in the expansion capacity of the chain and the water storage capacity in its pores³⁸.

These behaviors also can be attributed to their molecular structure and morphology⁷, because the pores among the polymer network decreased, and the number of pores increased when the silica concentration used in the hydrogel preparation increased. However, it is important to highlight that with increasing silica concentration in the

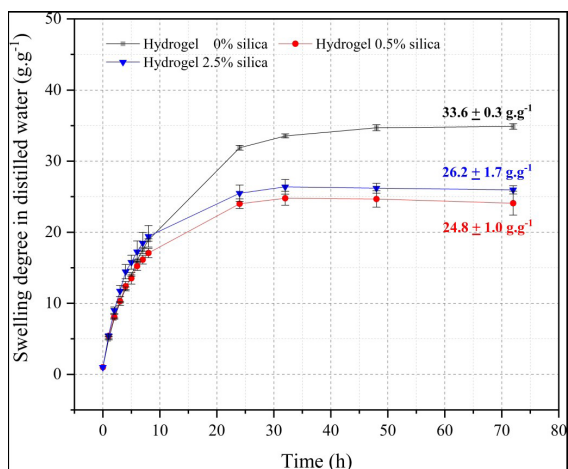


Figure 2. Swelling curves as a function of time for hydrogels with different Silica concentrations in distilled water.

polymer matrix, there is an increase in the swelling degree. According to Jia et al.³⁸, this behavior is related to the fact that the silica particles agglomerate resulting in a decrease in the crosslinking density and consequently increasing the SDeq as the silica content increases. Bose et al.¹⁵ explain that it occurs because the silica particles are physically confined in the polymer network, such surface adsorption would manifest as an increase in absorption capacity.

Thus, hydrogels with large pores have more significant interaction with water molecules, resulting in large water uptake.

3.2. Kinect parameters

The mechanism of water absorption is associated with the diffusional exponent (n) and the diffusion speed of the solvent (k)⁴¹. The mechanism can occur in four different ways: where $n < 0.45$, the mechanism occurs by *Fickian* diffusion; when $n = 0.89$, the diffusion occurs by case II-transport; in other words, this mechanism is governed by polymer swelling (chains relaxation); for $0.45 < n < 0.89$, the diffusion mechanism is classified as anomalous transport (*non-Fickian* diffusion), that is, the combination of the two previous; and when $n > 0.89$ corresponds to super case II-transport^{42,43}. Changes in kinetic parameters as a function of silica concentration are shown in Table 1.

All composites presented values of n around 0.45. The water absorption mechanism of all hydrogels has anomalous behavior, that is when the diffusion times and relaxation rates of the chains are comparable. Thus, both the sorption and transport of molecules are affected by the presence of pre-existing microcavities in the polymeric matrix^{44,45}. However, the increase in the silica concentration in the composite matrices modifies the water absorption, tending to *Fickian* transport, where the diffusion rate is much slower than the relaxation time of the polymer chain. This relaxation time is the time it takes for the chain to settle, that is, to come into balance with the presence of the solute or solvent.

3.3. Fourier transform infrared spectroscopy (FTIR)

Figure 4 shows the FTIR characterization of silica samples and composite hydrogels containing different proportions of silica.

As for the (a) silica spectra, a peak was observed around 3443 cm^{-1} , which is attributed to the groups $-\text{OH}$, the stretching vibrations belonging to the Si-O-Si groups are related to the peaks 1384 and 1120 cm^{-1} . The bands at 874 and 479 cm^{-1} are related to Si-OH stretching vibrations and Si-O-Si angular deformations, respectively⁴⁶⁻⁴⁸.

In the hydrogel spectra (b) it is possible to observe bands at 3188 and 2924 cm^{-1} , referring to the stretching vibrations of the $-\text{NH}$ and $-\text{CH}_3$ groups, respectively. The bands at 1670 and 1353 cm^{-1} can be assigned to the

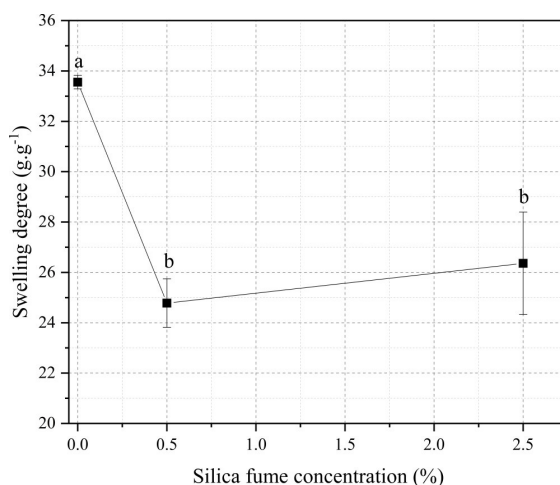


Figure 3. Effect of the amount of silica on the equilibrium swelling degree. Average with their respective standard deviation values, followed by equal letters do not differ statistically from each other following the Tukey test with a 95% confidence level.

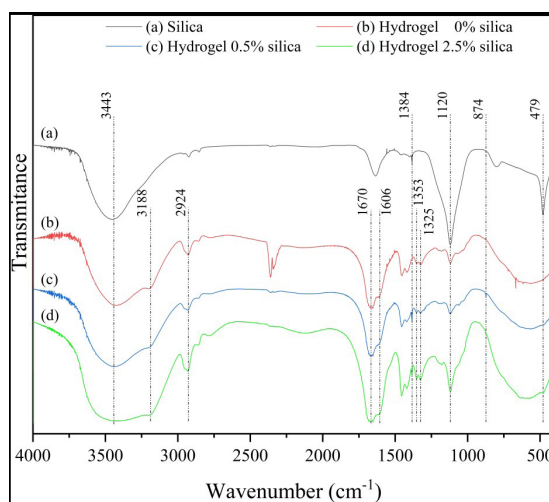


Figure 4. FTIR spectra of silica, pure hydrogel (0%), and composite hydrogel containing 0.5 and 2.5% of silica.

Table 1. Values of k and n obtained for different concentrations of silica in the hydrogels swelled in distilled water.

Silica concentration (% w/w)	Distilled Water			
	SD_{eq} (g.g ⁻¹)	n	k (h ⁻¹)	R^2
0	33.6 ± 0.3 ^a	0.43 ± 0.02 ^a	0.30 ± 0.03 ^a	0.98
0.5	26.2 ± 1.7 ^b	0.42 ± 0.10 ^a	0.27 ± 0.02 ^a	0.94
2.5	24.8 ± 1.0 ^b	0.44 ± 0.10 ^a	0.26 ± 0.02 ^a	0.95

Average with their respective standard deviation values, followed by equal letters do not differ statistically from each other following the Tukey test with a 95% confidence level

stretching vibration of the carbonyl group (C=O) and C-N. The bands at 1606 and 1420 cm^{-1} belong to the stretching strain of the COO^- groups, and at 1325 cm^{-1} to the axial strain of the $-\text{OH}$ groups.

In the region near 1456 cm^{-1} , the presence of a band associated with the vibration of secondary amines^{12,49-51} was observed. Thus, in the hydrogel spectra, it is possible to observe groupings of the presence of AAm, CMC, and MBAAm, indicating the formation of the PAAM-CMC polymeric matrix.

Regarding the spectra of the hydrogel compounds at different concentrations of 0.5% (c) and 2.5% (d) of silica, it was possible to observe the formation and intensification

of characteristic bands of silica in regions approximating 1384, 1120 and 479 cm^{-1} , thus evidencing the formation of the composite as expected. Similar behavior was also observed by Zareie et al.⁵² on the FTIR spectra of composite hydrogel containing polyacrylamide and silica.

3.4. X-ray diffraction (XRD)

The XRD was used to analyze the structure and crystallinity of the composite hydrogel. As shown in Figure 5, the diffraction patterns da silica indicate an amorphous SiO_2 structure at approximately $2\theta = 22^\circ$ ^{46,47,53,54}.

The diffraction pattern of pure hydrogel demonstrates an amorphous halo em $2\theta = 21.20^\circ$, which was already expected due to the irregular crosslinking of a polymer matrix chain. The composite hydrogel containing 0.5 and 2.5% of silica also has an amorphous structure. However, the diffractograms of the composite hydrogel show a shift from the amorphous halo to larger (2θ) diffraction angles (22.58°) and a lower overall signal intensity. Such effects may be related to the presence of silica in the hydrogel matrix.

3.5. Scanning electron microscopy (SEM)

SEM analyses allow for the characterization of the morphology of the structure of the polymeric matrix and the evaluation of the effects of additions on the different concentrations of silica. From Figure 6a, it was possible to observe that pure hydrogel is a structure with large pore spaces, a well-defined format, and heterogeneous pore sizes.

Similar structures of hydrogels constituted by PAAM and CMC were observed by Nascimento et al.¹⁰, Chen et al.⁵⁵, and Li et al.⁵⁶. However, the SEM micrograph of composite hydrogels with different silica concentrations of 0.5, and 2.5% (Figure 6b and 6c) show that with increasing addition of silica,

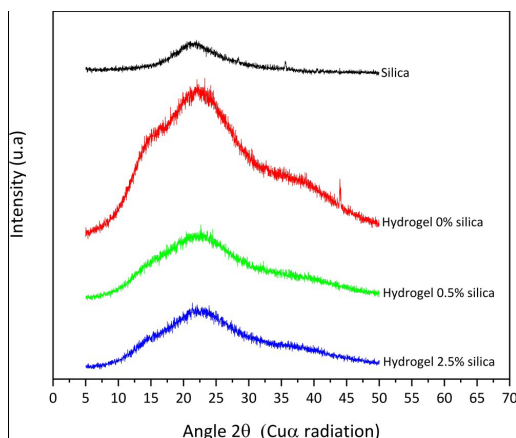
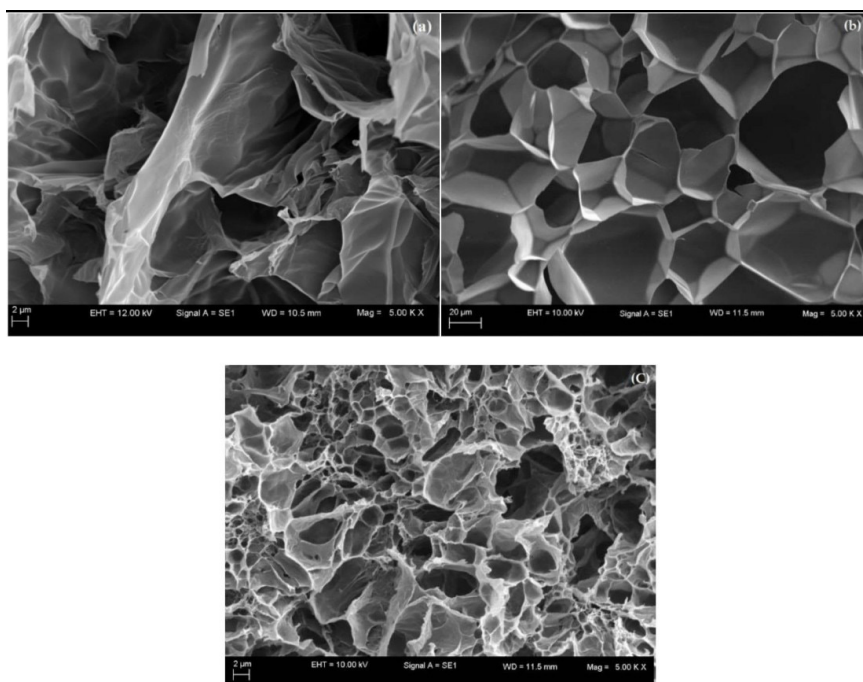


Figure 5. XRD of silica, pure hydrogel (0%), and composite hydrogel with 0.5 and 2.5% of silica.



Figures 6. SEM images of the composite hydrogels containing different proportions of silica 0 (a), 0.5 (b), and 2.5% (c).

provides a decrease in pore size compared to the pure hydrogel. This is because silica can form intermolecular and intramolecular bonds with the polymeric matrix⁵⁷. Therefore, the presence of silica probably increased the crosslinking density of the composite hydrogels, and decrease in free spaces to store water molecules, resulting in a reduction in water absorption, as can be observed in the swelling degree results. Thus, as described by Xu et al.⁵⁷ and Olad et al.⁵⁸, the presence of SiO₂ nanoparticles promotes excessive crosslinking of the polymeric chain, providing denser polymeric structures with smaller pores.

4. Conclusions

This study investigated the effect of hydrogels prepared from different concentrations of silica (0, 0.5, and 2.5% wt/wt acrylamide). The main findings are listed as follows:

- PAAm, CMC, and silica composite hydrogel were successfully synthesized via free-radical polymerization. Thus, PAAm, CMC and silica composite hydrogel can be considered a multicomponent system, because they were produced with two different polymers. Thus, these hydrogels can be classified as semi-IPNs systems, since only the PAAm is crosslinked and entangled with the non-crosslinked CMC polysaccharide in the polymer network.

- FTIR indicated that silica was incorporated successfully into the polymeric matrix, because it was possible to observe the formation and intensification of characteristic bands of silica in regions approximating 1384, 1120 and 479 cm⁻¹, thus evidencing the formation of the composite as expected. It is also emphasized that, in the hydrogel spectra, it is possible to identify AAm, CMC, and MBAAm specific groups, indicating the formation of the PAAm-CMC polymeric matrix.

- The presence of silica interferes directly with their water absorption because silica increased the crosslink density of the hybrid composites, decreasing the free spaces to accommodate water molecules, and this can cause a reduction in the expansion capacity of the chain and the water storage capacity in its pores. The reduction of SD_{eq} for hybrid hydrogels (0.50 and 2.5% silica) was 26.19% and 22.02%, respectively, when compared with PAAm+CMC hydrogel. This result was confirmed by SEM images.

- The analysis of the kinetic properties showed that there were no significant variations in the absorption velocity with the increase of the silica concentration. The values of the diffusion exponents were minor than 0.43, indicating that the release mechanism observed tends to a Fickian behavior;

- The X-ray analysis allowed us to observe that the samples analyzed have amorphous structures. It also observed a displacement of the diffraction angle (2θ) and a very broad halo with low intensity, evidencing the presence of silica in the polymer matrix.

In general, these results suggest an effective interaction between the silica and hydrogel matrix. Thus, the development of hybrid biodegradable hydrogels is relevant because the improvement of the properties of these composites expands their potential applications in different areas.

5. Acknowledgements

The authors would like to thank to the Federal Institute of Education, Science and Technology of Sao Paulo

(IFSP) and Sao Paulo State University (UNESP), São Paulo Research Foundation (FAPESP) (2018/18697-1; 2013/03643-0; 2013/07296-2), National Council for Scientific and Technological Development (CNPq) (MCTIC Grant #406973/2022-9 through INCT/Polysaccharides – National Technology-Science Institute for Polysaccharides; MRM 315513/2021-7; FAA 312414/2018-8; 316174/2021-1). This study was financed in part by the Coordenação de Aperfeiçoamento de Pessoal de Nível Superior – Brasil (CAPES) – “Finance Code 001”.

6. Data Availability

The raw/processed data required to reproduce these findings cannot be shared at this time as the data also forms part of an ongoing study.

7. References

1. Mahinroosta M, Farsangi ZJ, Allahverdi A, Shakoobi Z. Hydrogels as intelligent materials: a brief review of synthesis, properties, and applications. *Mater Today Chem.* 2018;8:42-55. <http://dx.doi.org/10.1016/j.mtchem.2018.02.004>.
2. Wahid F, Zhao XJ, Jia SR, Bai H, Zhong C. Nanocomposite hydrogels as multifunctional systems for biomedical applications: current state and perspectives. *Compos, Part B Eng.* 2020;200:108208. <http://dx.doi.org/10.1016/j.compositesb.2020.108208>.
3. Dragan ES, Apopei DF. Synthesis and swelling behavior of pH-sensitive semi-interpenetrating polymer network composite hydrogels based on native and modified potatoes starch as potential sorbent for cationic dyes. *Chem Eng J.* 2011;178:252-63. <http://dx.doi.org/10.1016/j.cej.2014.01.065>.
4. Myung D, Waters D, Wiseman M, Duhamel PE, Noolandi J, Ta CN et al. Progress in the development of interpenetrating polymer network hydrogels. *Polym Adv Technol.* 2008;19(6):647-57. <http://dx.doi.org/10.1002/pat.1134>.
5. Klempner D, Sperling LH, Utracki LAA. *Interpenetrating polymer networks.* Washington, DC: American Chemical Society; 1994. <http://dx.doi.org/10.1021/ba-1994-0239.ch001>.
6. Moura MRD, Rubira AF, Muniz EC. Semi-IPN hydrogels based on alginate-Ca²⁺ network and PNIPAAm: hydrophilic, morphological and mechanical properties. *Polimeros.* 2008;18:132-7. <http://dx.doi.org/10.1590/S0104-14282008000200010>.
7. Farzarian K, Teixeira KP, Rocha P, Carneiro LDS, Ghahremaninezhad A. The mechanical strength, degree of hydration, and electrical resistivity of cement paste modified with superabsorbent polymers. *Constr Build Mater.* 2016;109:156-65. <http://dx.doi.org/10.1016/j.conbuildmat.2015.12.082>.
8. Ullah F, Othman MBH, Javed F, Ahmad Z, Akil HM. Classification, processing, and application of hydrogels: a review. *Mater Sci Eng C.* 2015;57:414-33. <http://dx.doi.org/10.1016/j.msec.2015.07.053>.
9. Matricardi P, Di Meo C, Coviello T, Hennink WE, Alhaique F. Interpenetrating polymer networks polysaccharide hydrogels for drug delivery and tissue engineering. *Adv Drug Deliv Rev.* 2013;65(9):1172-87. <http://dx.doi.org/10.1016/j.addr.2013.04.002>.
10. Nascimento DWS, Moura MR, Mattoso LHC, Aouada FA. Hybrid biodegradable hydrogels obtained from nanoclay and carboxymethylcellulose polysaccharide: hydrophilic, kinetic, spectroscopic, and morphological properties. *J Nanosci Nanotechnol.* 2017;17(1):821-7. <http://dx.doi.org/10.1166/jnn.2017.12664>.
11. Brito CWQ, Rodrigues FHA, Fernandes MVS, Silva LRD, Ricardo NMPS, Feitosa JPA et al. Synthesis and characterization of poly(acrylamide-co-acrylate) and kaolin hydrogel composites: effect of the constitution of different kaolins from northeastern

- Brazil. *Quim Nova*. 2013;36(1):40-5. <http://dx.doi.org/10.1590/S0100-40422013000100008>.
12. Rudzinski WE, Dave AM, Vaishnav UH, Kumbar SG, Kulkarni AR, Aminabhavi TM. Hydrogels as controlled release devices in agriculture. *Des Monomers Polym*. 2002;5(1):39-65. <http://dx.doi.org/10.1163/156855502760151580>.
 13. Zohourian-Mehr MJAD, Kabiri K. Superabsorbent polymer materials: a review. *Iran Polym J*. 2008;17(6):451-77.
 14. Hasholt MT, Jensen OM, Kovler K, Zhutovsky S. Can superabsorbent polymers mitigate autogenous shrinkage of internally cured concrete without compromising the strength? *Constr Build Mater*. 2012;31:226-30. <http://dx.doi.org/10.1016/j.conbuildmat.2011.12.062>.
 15. Bose B, Davis CR, Erk KA. Microstructural refinement of cement paste internally cured by polyacrylamide composite hydrogel particles containing silica fume and nanosilica. *Cement Concr Res*. 2021;143:106400. <http://dx.doi.org/10.1016/j.cemconres.2021.106400>.
 16. Davis CR, Bose B, Alcaraz AM, Martinez CJ, Erk KA. Altering the crosslinking density of polyacrylamide hydrogels to increase swelling capacity and promote calcium hydroxide growth in cement voids. In: Boshoff WP, Combrinck R, Mechtcherine V, Wyrzykowski M, editors. 3rd International Conference on the Application of Superabsorbent Polymers (SAP) and Other New Admixtures Towards Smart Concrete. Cham: Springer; 2020. p. 20-8. http://dx.doi.org/10.1007/978-3-030-33342-3_3.
 17. Rizwan M, Gilani SR, Durani AI, Naseem S. Materials diversity of hydrogel: synthesis, polymerization process and soil conditioning properties in agricultural field. *J Adv Res*. 2021;33:15-40. <http://dx.doi.org/10.1016/b978-0-12-816421-1.00013-6>.
 18. Bortolin A, Aouada FA, Mattoso LHC, Ribeiro C. Nanocomposite PAAm/methyl cellulose/montmorillonite hydrogel: evidence of synergistic effects for the slow release of fertilizers. *J Agric Food Chem*. 2013;61(31):7431-9. <http://dx.doi.org/10.1021/jf401273n>.
 19. Stealey ST, Gaharwar AK, Pozzi N, Zustiak SP. Development of nanosilicate-hydrogel composites for sustained delivery of charged biopharmaceutics. *ACS Appl Mater Interfaces*. 2021;13(24):27880-94. <http://dx.doi.org/10.1021/acsami.1c05576>.
 20. Lee YC, Vinh VT, Duckshin P. Hydrogel applications for adsorption of contaminants in water and wastewater treatment. *Environ Sci*. 2018;25:24569-99. <http://dx.doi.org/10.1007/s11356-018-2605-y>.
 21. Pourjavadi A, Tehrani ZM, Salimi H, Banazadeh A, Abedini N. Hydrogel nanocomposite based on chitosan-g-acrylic acid and modified nanosilica with high adsorption capacity for heavy metal ion removal. *Iran Polym J*. 2015;24:725-34. <http://dx.doi.org/10.1007/s13726-015-0360-1>.
 22. Fernandes RS, Tanaka FN, Angelotti AM, Ferreira CR Jr, Yonezawa UG, Watanuki A Fo et al. Properties, synthesis, characterization and application of hydrogel and magnetic hydrogels: a concise review. In: Gogaiah S, Singh HB, Fraceto LF, Lima R, editors. *Advances in nano-fertilizers and nano-pesticides in agriculture: a smart delivery system for crop improvement*. Oxford: Elsevier; 2021. p. 437-57. (Woodhead Publishing Series in Food Science, Technology and Nutrition). <https://doi.org/10.1016/B978-0-12-820092-6.00017-3>.
 23. Camani PH, Toguchi JPM, Fiori APSM, Rosa DS. Impact of unmodified (PGV) and modified (Cloisite20A) nanoclays into biodegradability and other properties of (bio)nanocomposites. *Appl Clay Sci*. 2020;186(1):105453. <http://dx.doi.org/10.1016/j.clay.2020.105453>.
 24. Krafcik MJ, Bose B, Erk K. Synthesis and characterization of polymer-silica composite hydrogel particles and influence of hydrogel composition on cement paste microstructure. *Adv Civ Eng Mater*. 2018;7(4):590-613. <https://doi.org/10.1520/ACEM20170144>.
 25. Ferreira CR Jr, Moura MR, Aouada FA. Synthesis and characterization of intercalated nanocomposites based on poly(methacrylic acid) hydrogel and nanoclay cloisite-Na+ for possible application in agriculture. *J Nanosci Nanotechnol*. 2017;17(8):5878-83. <http://dx.doi.org/10.1166/jnn.2017.13843>.
 26. Palmese LL, Thapa RK, Sullivan MO, Kiick KL. Hybrid hydrogels for biomedical applications. *Curr Opin Chem Eng*. 2019;24:143-57. <http://dx.doi.org/10.1016/j.coche.2019.02.010>.
 27. Panpinit S, Pongsomboon SA, Keawin T, Saengsuwan S. Development of multicomponent interpenetrating polymer network (IPN) hydrogel films based on 2-hydroxyethyl methacrylate (HEMA), acrylamide (AM), polyvinyl alcohol (PVA) and chitosan (CS) with enhanced mechanical strengths, water swelling and antibacterial properties. *React Funct Polym*. 2020;156:104739. <http://dx.doi.org/10.1016/j.reactfunctpolym.2020.104739>.
 28. Caulfield MJ, Qiao GG, Solomon DH. Some aspects of the properties and degradation of polyacrylamides. *Chem Rev*. 2002;102(9):3067-84. <http://dx.doi.org/10.1021/cr010439p>.
 29. Yang C, Yin T, Suo Z. Polyacrylamide hydrogels. I. Network imperfection. *J Mech Phys Solids*. 2019;131:43-55. <http://dx.doi.org/10.1016/j.jmps.2019.06.018>.
 30. Paulino AT, Belfiore LA, Kubota LT, Muniz EC, Tambourgi EB. Efficiency of hydrogels based on natural polysaccharides in the removal of Cd²⁺ ions from aqueous solutions. *Chem Eng J*. 2011;168(1):68-76. <http://dx.doi.org/10.1016/j.cej.2010.12.037>.
 31. Ray SS, Bousmina M. Biodegradable polymers and their layered silicate nanocomposites: in greening the 21st century materials world. *Prog Mater Sci*. 2005;50(8):962-1079. <http://dx.doi.org/10.1016/j.pmatsci.2005.05.002>.
 32. Yang J, Han CR, Duan JF, Xu F, Sun RC. In situ grafting silica nanoparticles reinforced nanocomposite hydrogels. *Nanoscale*. 2013;5(22):10858-63. <http://dx.doi.org/10.1039/C3NR04252A>.
 33. Xing W, Tang Y. On mechanical properties of nanocomposite hydrogels: searching for superior properties. *Nano Materials Science*. 2022;4(2):83-96. <http://dx.doi.org/10.1016/j.nanoms.2021.07.004>.
 34. Aouada FA. Synthesis and characterization of methylcellulose polysaccharide and polyacrylamide hydrogels for controlled release of pesticides [thesis]. São Carlos: Universidade Federal de São Carlos; 2009.
 35. Santos JCD, Tashima MM, Moura MR, Aouada FA. Obtainment of hybrid composites based on hydrogel and Portland cement. *Quim Nova*. 2016;39:124-9. <http://dx.doi.org/10.5935/0100-4042.20160005>.
 36. Riger PL, Peppas NA. A simple equation for description of solute release II. Fickian and anomalous release from swellable devices. *J Control Release*. 1987;5(1):37-42. [http://dx.doi.org/10.1016/0168-3659\(87\)90035-6](http://dx.doi.org/10.1016/0168-3659(87)90035-6).
 37. Wang H, Wang Z, Zhu B. Preparation and properties of new non-loading and superhigh ammonium nitrate loading hydrogels. *React Funct Polym*. 2007;67(3):225-32. <http://dx.doi.org/10.1016/j.reactfunctpolym.2006.11.004>.
 38. Jia Y, Chen J, Liu W, Yin D. Construction of highly stretchable silica/polyacrylamide nanocomposite hydrogels through hydrogen bond strategy. *J Polym Res*. 2019;26(119):1-9. <http://dx.doi.org/10.1007/s10965-019-1761-1>.
 39. Shao C, Chang H, Wang M, Xu F, Yang J. High-strength, tough, and self-healing nanocomposite physical hydrogels based on the synergistic effects of dynamic hydrogen bond and dual coordination bonds. *ACS Appl Mater Interfaces*. 2017;9(34):28305-18. <http://dx.doi.org/10.1021/acsami.7b09614>.
 40. Li P, Siddaramaiah, Kim NH, Yoo GH, Lee JH. Poly(acrylamide/laponite) nanocomposite hydrogels: swelling and cationic dye adsorption properties. *J Appl Polym Sci*. 2008;111(4):1786-98. <http://dx.doi.org/10.1002/app.29061>.
 41. Fernandes RS, Tanaka FN, Moura MR, Aouada FA. Development of alginate/starch-based hydrogels crosslinked with different ions: hydrophilic, kinetic and spectroscopic properties. *Mater*

- Today Commun. 2019;21:100636. <http://dx.doi.org/10.1016/j.mtcomm.2019.100636>.
42. Aderibigbe BA, Varaprasad K, Sadiku ER, Ray SS, Mbianda XY, Fotsing MC et al. Kinetic release studies of nitrogen-containing bisphosphonate from gum acacia crosslinked hydrogels. *Int J Biol Macromol.* 2015;73:115-23. <http://dx.doi.org/10.1016/j.ijbiomac.2014.10.064>.
 43. Justo-Reinoso I, Caicedo-Ramirez A, Subrar WV III, Hernandez MT. Fine aggregate substitution with acidified granular activated carbon influences fresh-state and mechanical properties of ordinary Portland cement mortars. *Constr Build Mater.* 2019;207(20):59-69. <http://dx.doi.org/10.1016/j.conbuildmat.2019.02.063>.
 44. Ibrahim S, Nawwar GAM, Sultan M. Development of bio-based polymeric hydrogel: green, sustainable and low cost plant fertilizer packaging material. *J Environ Chem Eng.* 2016;4(1):203-10. <http://dx.doi.org/10.1016/j.jece.2015.10.028>.
 45. Aalaie J, Vasheghani-Farahani E, Rahmatpour A, Semsarzadeh MA. Effect of montmorillonite on gelation and swelling behavior of sulfonated polyacrylamide nanocomposite hydrogels in electrolyte solutions. *Eur Polym J.* 2008;44(7):2024-31. <http://dx.doi.org/10.1016/j.eurpolymj.2008.04.031>.
 46. Kocak YA. Study on the effect of fly ash and silica fume substituted cement paste and mortars. *Sci Res Essays.* 2010;5(9):990-8.
 47. Ekrem K, Hayrunnisa N. Adsorptive removal of acid fuchsin dye using by-product silica fume and laccase-modified silica fume. *Iranian. J Chem Chem Eng.* 2021;40(2):551-64. <http://dx.doi.org/10.30492/ijcce.2019.37339>.
 48. Khater HM, Gharieb M. Synergetic effect of nano-silica fume for enhancing physicochemical properties and thermal behavior of MK-geopolymer composites. *Constr Build Mater.* 2022;350:128879. <http://dx.doi.org/10.1016/j.conbuildmat.2022.128879>.
 49. Tanaka FN, Ferreira CR Jr, Moura MR, Aouada FA. Water absorption and physicochemical characterization of navel zeolite-PMAA-co-PAAm nanocomposites. *J Nanosci Nanotechnol.* 2018;18(10):7286-95. <http://dx.doi.org/10.1166/jnn.2018.15515>.
 50. Pfeifer M, Andrade FAC, Santos RB, Aouada FA, Ribeiro C. Effect of different surface-charged lamellar materials on swelling properties of nanocomposite hydrogels. *J Polym Environ.* 2021;29:3311-23. <http://dx.doi.org/10.1007/s10924-021-02120-7>.
 51. Calesco MAF, Watanuki A Fo, Moura MR, Aouada FA. Effects of addition of hybrid nanocomposite based on polysaccharide hydrogel and nanoclay on the fresh and hardened properties of cementitious mortars. *Ceramica.* 2022;68(385):97-107. <http://dx.doi.org/10.3390/polym14214564>.
 52. Zareie C, Bahramian AR, Sefti MV, Salehi MB. Network strength relationship and performance improvement of polyacrylamide hydrogel using nano-silica; with regards to application in oil wells conditions. *J Mol Liq.* 2019;278:512-20. <http://dx.doi.org/10.1016/j.molliq.2019.01.089>.
 53. Li Y, Li T, Jin Z. Stabilization of Fe0 nanoparticles with silica fume for enhanced transport and remediation of hexavalent chromium in water and soil. *J Environ Sci.* 2011;23(7):1211-8. [http://dx.doi.org/10.1016/S1001-0742\(10\)60534-7](http://dx.doi.org/10.1016/S1001-0742(10)60534-7).
 54. Shukla N, Gupta V, Rawat AS, Gahlot VK, Shrivastava S, Rai PK. 2,4-Dinitrotoluene (DNT) and 2, 4, 6-Trinitrotoluene (TNT) removal kinetics and degradation mechanism using zero-valent iron-silica nanocomposite. *J Environ Chem Eng.* 2018;6(4):5196-203. <http://dx.doi.org/10.1016/j.jece.2018.08.018>.
 55. Chen C, Li Y, Qian C, Liu X, Yang Y, Han L et al. Carboxymethyl cellulose assisted PEDOT in polyacrylamide hydrogel for high performance supercapacitors and self-powered sensing system. *Eur Polym J.* 2022;179:111563. <http://dx.doi.org/10.1016/j.eurpolymj.2022.111563>.
 56. Li Y, Yang Y, Liu X, Yang Y, Wu Y, Han L et al. Flexible self-powered integrated sensing system based on a rechargeable zinc-ion battery by using a multifunctional polyacrylamide/carboxymethyl chitosan/LiCl ionic hydrogel. *Colloids Surf A Physicochem Eng Asp.* 2022;648:129254. <http://dx.doi.org/10.1016/j.colsurfa.2022.129254>.
 57. Xu P, Shang Z, Yao M, Ke Z, Li X, Liu P. Molecular insights on the mechanical properties of double-network hydrogels reinforced by covalent compositing with silica-nanoparticles. *J Mol Liq.* 2022;368:120611. <http://dx.doi.org/10.1016/j.molliq.2022.120611>.
 58. Olad A, Zebhi H, Salari D, Mirmohseni A, Reyhanitabar A. Synthesis, characterization, and swelling kinetic study of porous superabsorbent hydrogel nanocomposite based on sulfonated carboxymethylcellulose and silica nanoparticles. *J Porous Mater.* 2018;25:1325-35. <http://dx.doi.org/10.1007/s10934-017-0543-6>.